

Article

Fabrication of Aluminum Alloy with Open-Channel and Columnar Structures through a Ceramic Fiber Template Method

Hideo Nakajima ^{1,2,3} 

¹ Institute for Lotus Materials Research Co., Ltd., 1-1-3-267 Umeda, Osaka 530-0001, Japan; nakajima@sanken.osaka-u.ac.jp

² Sumitomo Precision Products Co., Ltd., Amagasaki 660-0891, Japan

³ SANKEN, Osaka University, Ibaraki 567-0047, Japan

Abstract: Aluminum alloys with open-channel and columnar structures were fabricated by casting the melt of aluminum alloys using a ceramic fiber template method. Stainless steel plates or wires coated with ceramic fibers impregnated by polyvinyl alcohol were used as cores. The cores were embedded in a melt of an aluminum alloy. After solidification, the ceramic fibers were macerated and became sodden by immersing the aluminum alloy ingots in water so that the plates or wires were easily removed by extraction forces as large as 5N, in other words, by pulling out them manually. Thus, an open-channel aluminum alloy was fabricated by a simple method. On the other hand, ceramic fiber blocks composed of ceramic fibers impregnated by polyvinyl alcohol were perforated by microdrills. Melts of aluminum alloy were cast in the holes by a vacuum suction method. The ceramic fibers were removed by immersing the ingots in water. Thus, a columnar-structured aluminum alloy was produced. Previous methods for the fabrication of open-channel metals necessitates a process to extract the metallic wires embedded in the solidified metals. However, the ceramic fiber template method does not require such an extraction process and thus is a very simple technique for the fabrication of open-channel metals, such as porous metals with rectangular holes and circular holes and columnar structures metals.

Keywords: aluminum; porous metals; columnar structure; ceramic fiber; solidification; directional holes; open-channel metals; casting



Citation: Nakajima, H. Fabrication of Aluminum Alloy with Open-Channel and Columnar Structures through a Ceramic Fiber Template Method.

Metals **2023**, *13*, 1914. <https://doi.org/10.3390/met13121914>

Academic Editors: Thomas Niendorf and Jiehua Li

Received: 15 October 2023

Revised: 4 November 2023

Accepted: 18 November 2023

Published: 21 November 2023



Copyright: © 2023 by the author. Licensee MDPI, Basel, Switzerland. This article is an open access article distributed under the terms and conditions of the Creative Commons Attribution (CC BY) license (<https://creativecommons.org/licenses/by/4.0/>).

1. Introduction

Porous, foamed, and cellular metals have various characteristics different from non-porous metals, such as an inherently low density and a large surface area. Therefore, these metals are expected to be utilized as lightweight materials, catalysts, electrodes, vibration and acoustic energy damping materials, impact energy absorption materials, and so on. Most of the porous, foamed, and cellular metals possess spherical or polyhedron pores [1]. On the other hand, lotus-type porous metals have long directional pores [2,3]. The former tends to exhibit isotropic features, while the latter tends to show anisotropic features. In the natural world, the most popular porous materials with directional holes are stems of plants, which are tissues that conduct water and nutrients through the plant body [4]. On the other hand, a prominent application of lotus-type porous metals is in heat sinks for cooling electronic devices [5]. The directional porous metals supply large surface areas in contact with the coolant and low pressure loss so that a high heat transfer rate is obtained. Thus, lotus-type porous copper is suitable for such heat sinks. Lotus-type porous copper is able to be fabricated by utilizing the solubility gap of hydrogen in between solid and melt [6–10]. Lotus-type porous aluminum is also desirable for lightweight heat sinks, which have a benefit for automobiles.

Utsunomiya et al. [11] and Vesenjok et al. [12,13] developed techniques for fabricating lotus-type porous copper by extruding wires of copper and aluminum and by the explosive

compaction of copper, respectively. Ide et al. demonstrated that lotus aluminum with long directional pores cannot be produced easily with the technique that utilizes the solubility gap because of hydrogen's low solubility in aluminum [14,15]. Thus, the challenge of producing aluminum with long open-channels that would lessen production costs and the weight of high-performance heat sinks remains.

Furthermore, there are a few perforation techniques for metals and alloys that do not involve melting the metallic matrix: mechanical drilling, electron beam processing, and laser ablation processing. Holes can be mechanically formed by drilling and removing material. However, several challenges make fabricating small holes difficult. (1) Drills with thicknesses of less than 1 mm in diameter are difficult to manufacture. (2) The drill bits are worn down through repeated mechanical drilling, and small drill bits break easily. Thus, creating perforations smaller than 1.0 mm in diameter is laborious, time-consuming, and costly [16].

Alternatively, Gillen and Moore adopted electron beam processing to make small holes [17]. In their method, an electron beam produced melting pools. The melt evaporated so that holes were formed. This technique should be conducted in a high-vacuum atmosphere, and thus, the technique is inefficient for practical application. The principle of laser beam processing is similar to that of electron beam processing. Gregory et al. used a focused laser beam in air to melt small points [18]. The technique is laborious and expensive. Furthermore, since aluminum is a lower-melting metal, the holes have an inverse tapered shape, as they widen due to increased melting during laser irradiation. These two conventional techniques can only create holes that are short, having aspect ratios at most as large as 10.

Two methods for fabricating open-channel metals and alloys that do not involve the evolution of gas pores by solidification have been reported. Hakamada et al. investigated the fabrication of open-channel copper by a space holder method [19]. Aluminum wires and copper powders were compacted by cold isostatic press. Then, the aluminum wires were removed by immersing the compact in NaOH aqueous solution for 48 h, and the compact was sintered.

Dunand et al. investigated porous titanium [20], its alloy [21], and NiTi [22]. Preform consisting of titanium powders containing steel space holders in the form of wires, spheres, and wire meshes were uniaxially cold-pressed to 350 MPa. Then, steel wires were removed from the sintered Ti-Fe composites in an electrolytic cell with the cathode (titanium sheet) and the anode (Ti-Fe composite) and a 10 vol.% acetic acid aqueous solution saturated with NaCl as the electrolyte. Full dissolution of the steel wire, which was 500 μm in diameter, was completed after about 10 h to form a cylindrical channel with a depth of ~ 8 mm and an aspect ratio of ~ 16 . Both of the techniques used powder sintering, which is expensive and not suitable for mass production at the commercial level. Furthermore, the removal of the wires embedded in sintered materials is time-consuming and laborious. An alternative method with time-saving and quick dissolution is desirable.

Haga and Fuse investigated the fabrication of open-channel aluminum and its alloys by pulling core-bars from a semisolid ingot [23–25]. Core-bars of mild steel with thickness ranging from 0.5 to 5.0 mm in diameter were settled in a metal mold. Then, molten metal was poured in the mold. The core-bars were pulled out from the metal at a designated temperature for the semisolid condition. The holes were collapsed at the temperature approaching the liquidus line temperature, where the solid fraction was low and the fluidity of the semisolid metal was high. The round shape of the cross-section of open-channel holes becomes more degraded as the temperature increases. When the temperature was higher, the viscosity of aluminum alloy decreased so that the extracted space was easily deformed. Unfortunately, since semisolid conditions must be utilized in the method, the pulling process at high temperatures is indispensable. In addition, the fabricated alloys in which the semisolid solution is formed are limited. Thus, a process that does not require semisolids is desirable.

On the other hand, Suzuki et al. developed a rod-dipping process to fabricate an open-channel aluminum alloy, A6061 [26–28]. Carbon rods with diameters of 2.0, 3.0, and 4.0 mm were dipped into a molten aluminum alloy. An ECAE (equal-channel angular extrusion) process was used to crush the carbon rods in order to remove the rods. Another method to remove the carbon rods is to evaporate carbon rods at high temperatures. In this method, pore sizes of less than 2 mm in diameter could not be fabricated because of the use of carbon rods, and the plastic-deforming process was indispensable. A method that does not use carbon rods or the plastic deforming process is required for low-cost performance.

Channel holes can also be fabricated by photoetching and diffusion-bonding techniques [29]. Thin foils made of stainless steel are chemically etched to the depth of several hundred μm . Non-etched parts are covered with photoresist films; only non-covered areas are etched. Several hundred sheets are diffusion-bonded by thermo-compression to produce open-channel stainless steel. Unfortunately, this technique cannot be applied to aluminum, because aluminum oxide is formed during thermo-compression, which prevents the bonding.

To overcome this problem, the present author developed an open-channel aluminum that was fabricated by extracting lubricated metallic wires embedded in solidified aluminum [30]. Stainless steel (SUS) wires are coated with boron nitride or alumina, which is used as lubricated layers. The wires are mounted into aluminum melt. After solidification, the wires are extracted by pulling the wires from the aluminum ingot so that elongated holes are formed. When fabricating the elongated holes, it is laborious to extract many wires one by one. If the extraction of many SUS wires is able to be carried out simultaneously, the fabrication of open-channel aluminum with many holes can be made time-saving and easy. For this purpose, one end of the SUS wires without lubricant coating are fastened onto a SUS plate, which is immersed into molten aluminum and then solidified. This whole jig is pulled out from the solidified ingot, and open-channel aluminum is produced.

Figure 1a shows a schematic drawing of the extraction procedure by gripping the whole jig and the aluminum ingot, and Figure 1b shows a photo of the extraction process using a tensile test machine. According to a previous investigation [31], it is known that the extraction force (tensile force) of n wires amounts to n times the extraction force per one wire. If n is a large number, a large extraction force should be necessary, so a large-capacity tensile test machine must be used, which affects the manufacturing cost, resulting in high cost performance. Therefore, a simple and easy extraction technique without the use of a large tensile test machine is desirable. Thereby, the present author came up with an idea if the following two conditions could be met:

- (1) The templates should be solid and inflexible when embedded in aluminum alloy melt;
- (2) Once solidified, the templates should be macerated by some solution to remove them so that the templates can be removed without any extraction force. Ceramic fibers and polyvinyl alcohol are chosen as the materials of the templates, and water is chosen as a solution to be satisfied. Although the fibers themselves are flexible, the fibers impregnated with polyvinyl alcohol harden and do not crook against the melt pressure when the aluminum alloy melt is poured into a crucible. The present research is conducted to simplify the manufacturing process by adopting such a ceramic fiber template method instead of the extraction method using the template of metallic wires coated with lubricant.

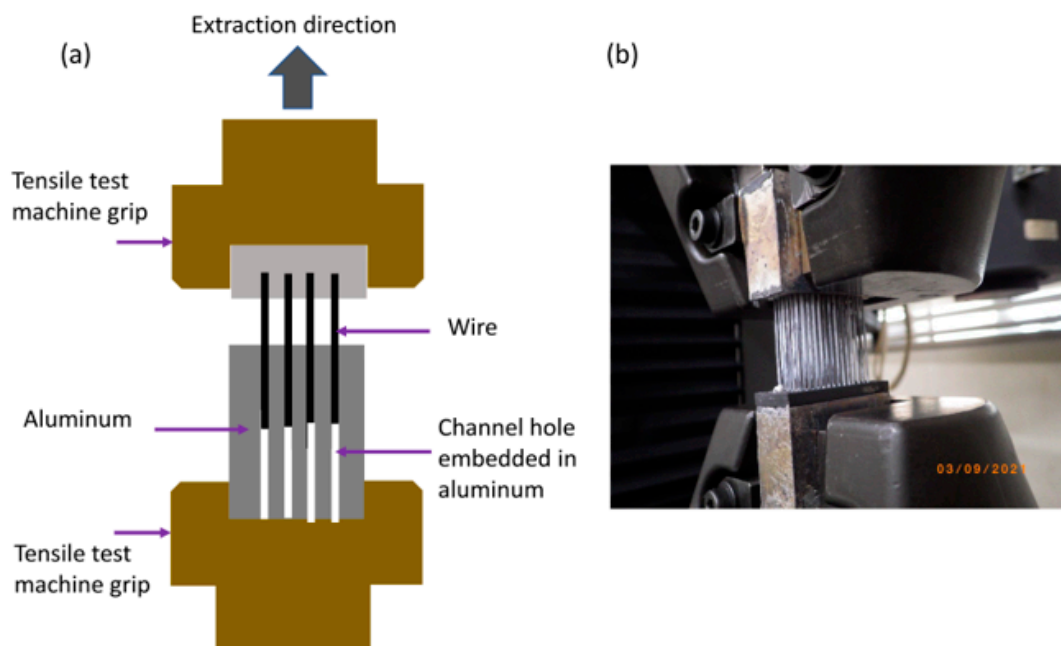


Figure 1. (a) Schematic drawing of wire extraction using a tensile test machine. The top end of SUS wires without coating the lubricant are fixed by aluminum, and other parts of the wires coated by the lubricant are extracted. (b) Both the top and the bottom are grasped, and the lubricated wires are extracted. The SUS wires are extracted by a tensile test machine. SUS wires: 1.0 mm in diameter and 85 mm in length, wire number 84. Lubricant: 90% BN and 10% MgH₂.

2. Materials and Fabrication Method

2.1. Fabrication of Open-Channel Aluminum Alloy

Open-channel aluminum alloys were fabricated by casting the melt of aluminum alloys using a ceramic fiber template method. The aluminum alloy AC4CH was used as the sample. The chemical composition is tabulated in Table 1.

Table 1. Chemical composition of aluminum alloy AC4CH (wt pct).

Si	Mg	Fe	Ni	Ti	P
6.92	0.42	0.07	0.01	0.12	0.0004

Cores were used as templates for open-channel rectangular holes or circular holes. The cores were made of ceramic fiber papers impregnated with polyvinyl alcohol. The ceramic fiber was composed of 70–80% SiO₂, 18–27% MgO, and an organic binder, whose bulk density is 210 kg m⁻³. The ceramic fiber paper impregnated with polyvinyl alcohol was dried and solidified by heating at 393 K for 10³ s. Both edges of the sheet-shaped cores were supported by graphite plates so that the sheets of the cores were arranged parallelly at even intervals, as shown in Figure 2a–c, which were set up in a graphite crucible. Figure 2a–c depicts the (a) top view, (b) front view, and (c) a schematic of the cut section of an open-channel aluminum alloy cut at the red line position in Figure 2a, respectively. Then, when aluminum melt was poured into the crucible, the sheets of the cores were deformed irregularly due to the melt pressure. The arrangement of the rectangular holes deviated from the ordered alignment as shown in Figure 2d. In order to prevent such deformation of the sheets of cores, reinforced materials, such as stainless steel (SUS) sheets or SUS wires, were introduced. Figure 3a,b shows the schematic drawings of cores reinforced by (a) SUS plates with thicknesses of 0.1 mm and (b) SUS wires with diameters of 0.8 mm, respectively. The reinforced materials were covered with the ceramic fiber paper impregnated by polyvinyl alcohol and dried by heating at the same temperature

and for the same duration as above. Since the cores were reinforced, no damage was suffered from any deformation due to the melt pressure.

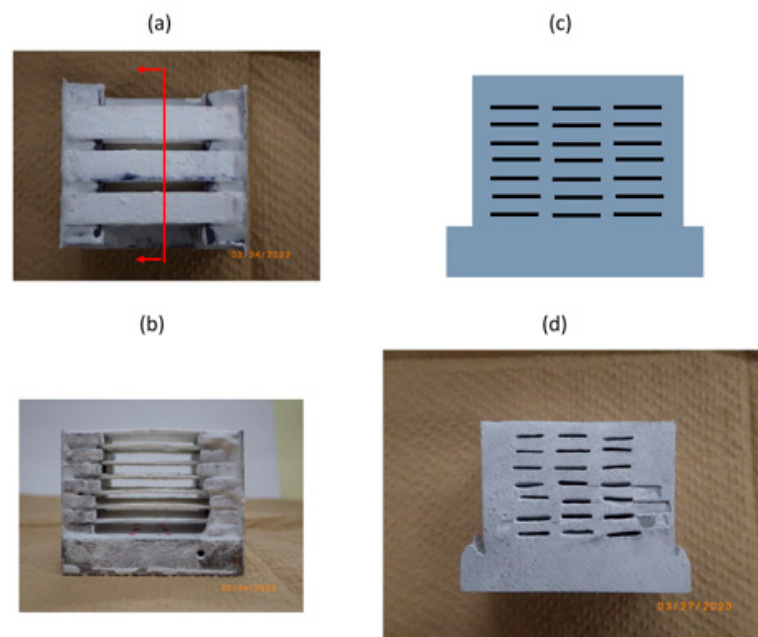


Figure 2. (a) Top view and (b) front view of 21 ceramic fiber papers impregnated with polyvinyl alcohol. Both edges are supported by graphite plates. (c) Schematic of cut section of open-channel aluminum alloy to be cut at the red line position in (a). (d) Actual cross-section of open-channel aluminum alloy. Fiber papers are deformed by melt pressure during casting. As a result, fabricated rectangular holes are distorted and are different from the predicted hole shapes.

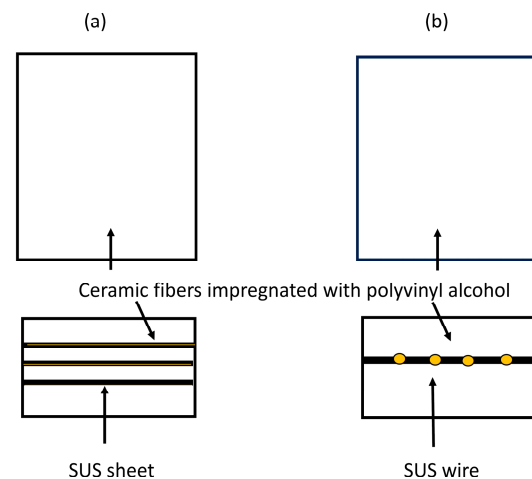


Figure 3. (a) Schematic drawing of ceramic fiber core sheets reinforced by SUS plates with thickness of 0.1 mm. (b) Schematic drawing of ceramic fiber core reinforced by SUS wires with diameter of 0.8 mm.

After casting and cutting both edges of the ingot to expose the fiber core, the solidified aluminum ingot was immersed into water. The ceramic fiber core absorbed water and was macerated to become sodden. The ceramic fiber was scattered in the form of small chips by blowing water or compressed air so that open-channel aluminum with directional holes was fabricated, as shown in Figure 4a.

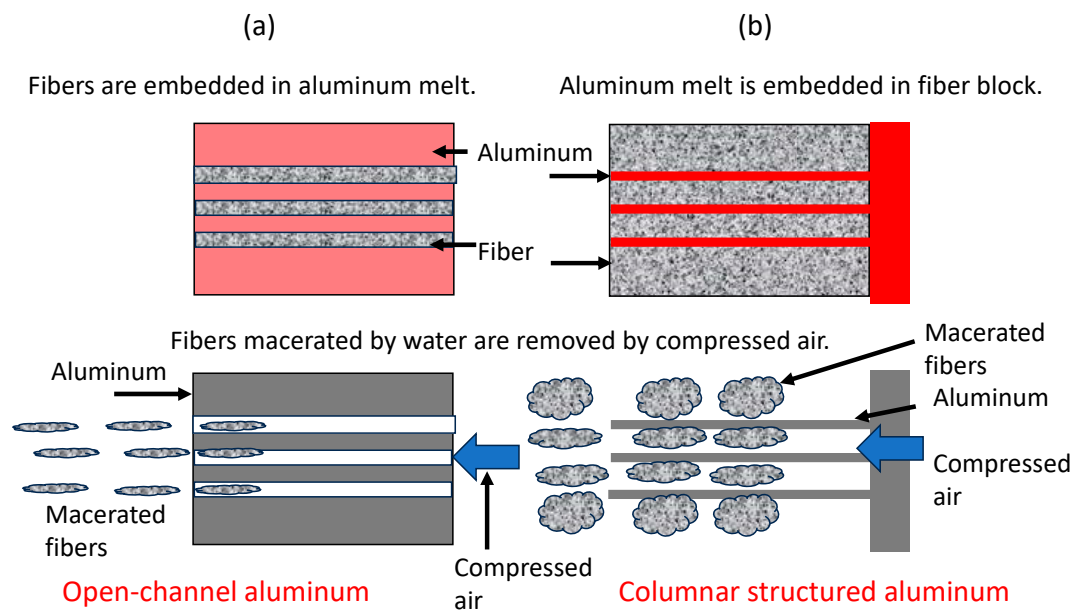


Figure 4. Schematic drawing of ceramic fiber template method. Fiber chips soddened with water are removed by compressed air. (a) Fabrication of open-channel aluminum and (b) fabrication of columnar-structured aluminum.

For the fabrication of the open-channel aluminum with circular holes, SUS wires were used as a reinforced material in order to prevent core deformation by melt pressure. The ceramic fibers were dissolved into polyvinyl alcohol and mixed. This solution was coated onto SUS wires with thicknesses of as much as 100–150 μm . The cores were embedded into the melt of the aluminum alloy, which was then solidified. Figure 5a's left-hand side and right-hand side show the cross-sectional view of the open-channel aluminum alloy and the appearance of the fiber-coated SUS wires, respectively. The surface of the wire was rough, and fabricated holes were distorted, which was attributed to the irregular coating of the fibered solution.

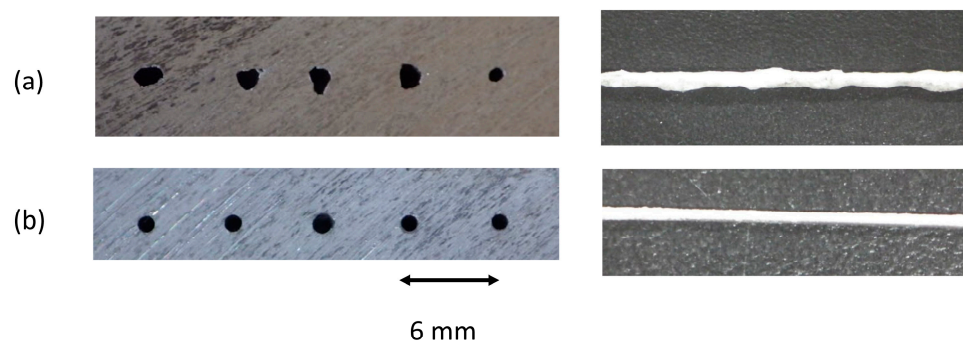


Figure 5. (left) The cross-sectional views of open-channel holes. (right) The appearance of fiber-coated SUS wires. (a) Coated with the mixture of ceramic fibers and polyvinyl alcohol. (b) Coated with the mixture of disassembled ceramic fibers and polyvinyl alcohol. The fine and smooth surface of the coated layers on SUS wires was obtained by disassembling ceramic fibers with polyvinyl alcohol.

The length of the fibers, which could be as long as 20 mm, was shortened and disassembled by mixing together with polyvinyl alcohol with a mixer. Furthermore, in order to improve adhesion between the SUS wire and ceramic fiber-coated layer, a mixture solution of 30–40% dimethylether, 20–25% methylene chloride, 15–20% alumina, 10–15% ethanol, 1–5% acetone, 1–5% glycerin, 1–5% cellulose gum, and 0.1–1% magnesium silicate mineral. (hereafter, called the adhesive) was first coated onto SUS wires. The coating thickness was 20–30 μm . Then, the fibered solution was coated with a thickness of 60–70 μm . These coated

SUS wires were mounted in a graphite crucible as the cores. Aluminum alloy melt degassed by argon bubbling was poured into the crucible (since the melt of the aluminum and its alloys are apt to absorb hydrogen, many micropores were evolved in solidified ingots. Hydrogen pores can be removed by argon gas bubbling. Argon bubbles are supplied in liquid aluminum and its alloys by inserting a nozzle whose side possesses holes for argon gas [32,33]). After the casting water was immersed into the ingot, the fibers and SUS wires were removed smoothly. Thus, an open-channel aluminum alloy was prepared. Figure 5b's left-hand side and right-hand side show the cross-sectional view of the open-channel aluminum alloy and the appearance of the disassembled fiber-coated SUS wire, respectively. The surface of the wire was improved to become smooth, and fabricated holes were circular, as was designed. In order to obtain such a smooth surface on the cores, the following two conditions are considered to be necessary:

- (1) The adhesive must improve the wettability of the mixture of ceramic fibers and polyvinyl alcohol to SUS wires;
- (2) Long ceramic fibers must be shortened and disassembled by mixing with polyvinyl alcohol using a mixer, thus causing them to change to minute ceramic fibers.

In order to measure the extraction force, which was the magnitude of force necessary to extract the SUS plates or wires, a tensile test machine, the Shimadzu Co., Ltd. (Kyoto, Japan) Autograph AG-100 kND, was used. The extraction velocity was 3 mm min^{-1} . The shape and the size of cross-sectional holes was observed with an optical microscope.

2.2. Fabrication of Columnar-Structured Aluminum Alloy

The columnar-structured aluminum alloy AC4CH was fabricated by casting the melt of the aluminum alloy using the ceramic fiber template method. Cores were used as templates. Ceramic fiber papers whose thickness was 1.0 mm were overlapped by twenty paper sheets, impregnated with polyvinyl alcohol, and dried at 393 K for 10^3 s to become solidified, thus fabricating a ceramic-fibered block. This fibered block was perforated by a high-speed precision micro-drilling machine, BDM-660 Nihon Seimitsu Kikai Kosaku Co., Ltd., Kawanishi, Hyogo, Japan. The size of the perforated directional holes were in the range from 0.6 mm to 3.6 mm in diameter. In order to cast the aluminum alloy melt into a graphite crucible, two kinds of setups of the core templates were adopted. As illustrated in Figure 6a, core templates were installed in a graphite crucible whose bottom was closed. This setup was used to fabricate the columns whose diameters were more than 2.0 mm. On the other hand, as shown in Figure 6b, core templates and porous ceramic sheets were settled in a graphite crucible whose bottom possessed a hole, which was evacuated for vacuuming with a rotary pump. When the perforated holes in the fiber block were thin, say less than 1.0 mm in diameter, the aluminum alloy melt could not penetrate into the thin holes because of the viscosity and surface tension of aluminum alloy melt. Therefore, a vacuum suction casting method was adopted to cause a certain negative pressure [34,35]. The aluminum alloy melt was forced into the thin holes under vacuuming at the bottom of crucible. During this penetration process, the aluminum alloy melt was solidified with high cooling rates. After the casting, the fibered blocks were dissolved and removed by immersion in water so that this columnar-structured aluminum alloy was fabricated as shown in Figure 4b.

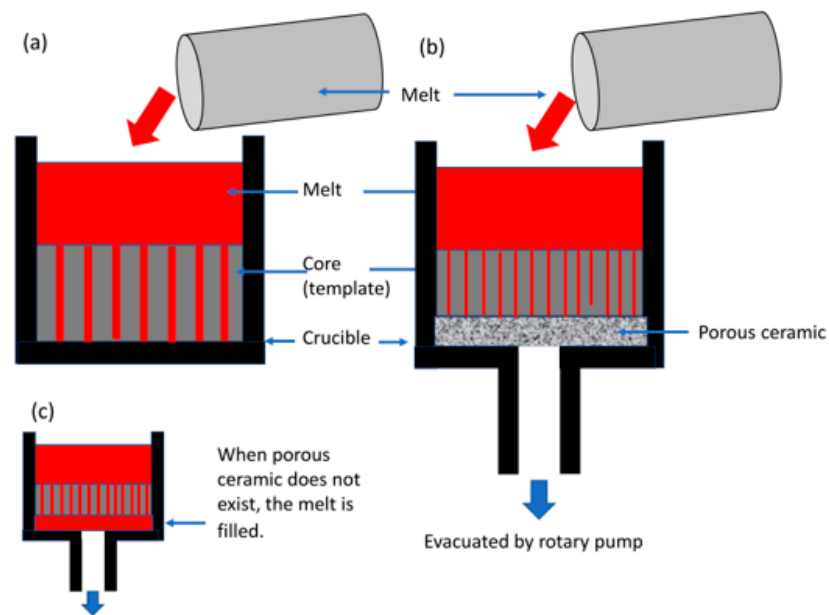


Figure 6. Schematic drawing of melting in crucibles. (a) Atmospheric casting to fabricate channel holes larger than 2 mm in diameter. (b) Vacuum suction casting by inserting porous ceramic to fabricate channel holes less than 2 mm in diameter. (c) Vacuum suction casting without inserting porous ceramic to fabricate channel holes less than 2 mm in diameter.

3. Results and Discussion

3.1. Fabrication of Open-Channel Aluminum Alloy

Figure 7a,b shows the cross-sectional views of the open-channel aluminum alloy perpendicular to the core sheets illustrated in Figures 3a and 3b, respectively. It was observed that the rectangular holes were not bent without any deformation due to the melt pressure. The rectangular holes were not deformed by inserting the reinforced SUS plates or wires into the fiber sheets, which were different from the result shown in Figure 2. Thus, the reinforcement of the cores by metallic plates or wires is effective.

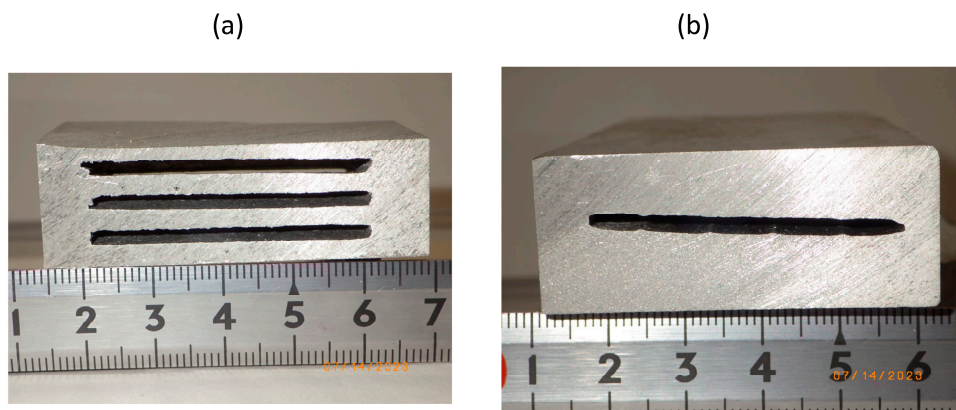


Figure 7. (a) Cross-sectional view of open-channel aluminum alloy perpendicular to the core sheets illustrated in Figure 3a. The thickness of the core sheet is 1.5 mm. (b) Cross-sectional view of open-channel aluminum alloy perpendicular to the core sheets illustrated in Figure 3b. The thickness of the core sheet is 2.0 mm.

Figure 8 shows the cross-sectional view of the open-channel aluminum alloy AC4CH perpendicular to the direction of SUS wires. The circular shape of the templates was kept as it was. SUS wires with a diameter of 1.96 mm were first coated with the adhesive and then coated with the mixture of ceramic fiber and polyvinyl alcohol disassembled

by the mixer. The thickness of the coated wires was 2.50 ± 0.15 mm in diameter. After casting, the thickness decreased to 2.13 ± 0.15 mm in diameter so that the thickness of the coated layer changed from $270 \mu\text{m}$ to $85 \mu\text{m}$. Thus, the coated layers were shrunk by $85/270 = 0.32\sim 0.3$. When the ceramic fiber and polyvinyl alcohol were mixed and disassembled by the mixer, microbubbles were formed so that the coated layers became porous. It is surmised that during casting, (1) the melt pressure causes the coated layers to inhale the micropores and/or (2) the stress due to solidification shrinkage decreases the number of the micropores. Thus, it is suggested that the shrinkage of the coated layers is attributed to the decrease in the porosity.

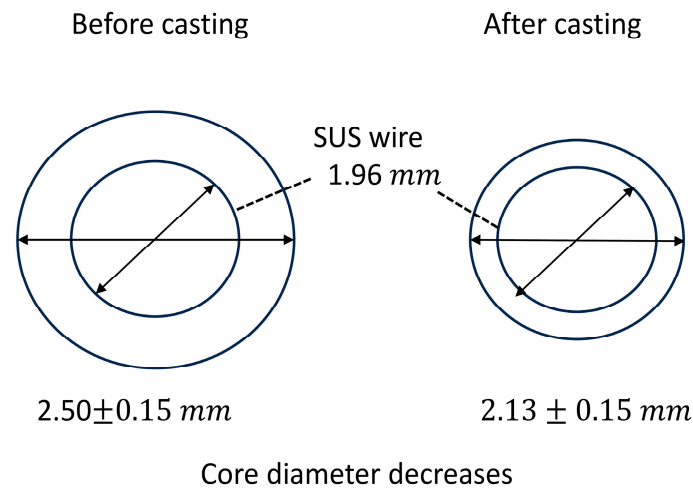


Figure 8. Cross-sectional views of template of open-channel aluminum alloy.

3.2. Fabrication of Columnar-Structured Aluminum Alloy

Figure 9 shows the columnar structure of the aluminum alloy AC4CH fabricated using the ceramic fiber template method. Holes perforated in the fiber block were utilized as templates for the columnar structure. As shown in Figure 9a, 97 holes with a diameter of 1.2 mm were drilled at a depth of 15 mm. After casting, 97 columns with a diameter of 1.2 mm and height of 15 mm should be elaborated as originally designed. However, only half of the columns were produced, while the other half of the columns failed, as shown in Figure 9b. Since the perforated holes were thin, it is considered that the melt of the aluminum alloy could not penetrate through these thin holes. Therefore, in order to fabricate columns less than 2.0 mm in diameter, the vacuum suction casting method was adopted.



Figure 9. (a) Ninety-seven holes perforated by a micro-drill in a ceramic fiber block. Height of block: 15 mm; holes: 1.2 mm in diameter. (b) Only half of the columns were fabricated by casting, and others were not.

Various sizes of columnar-structured aluminum alloys were fabricated. The columns shown in Figure 10a–c are cantilever-type columns, which were fabricated by a template

setup, as illustrated in Figure 6b. On the other hand, columns attached by aluminum alloy plates at the top and bottom were also fabricated, as shown in Figure 10d–f; these were produced by a template setup, as shown in Figure 6c. According to the application, either type of columnar structure should be selected. For example, if this columnar structure is utilized as a microchannel heat sink, one side faces the coolant and the other side faces the heating area, such as joule-heated electronic devices. In this case, a columnar structure attached by aluminum alloy plates at the top and bottom is desirable.

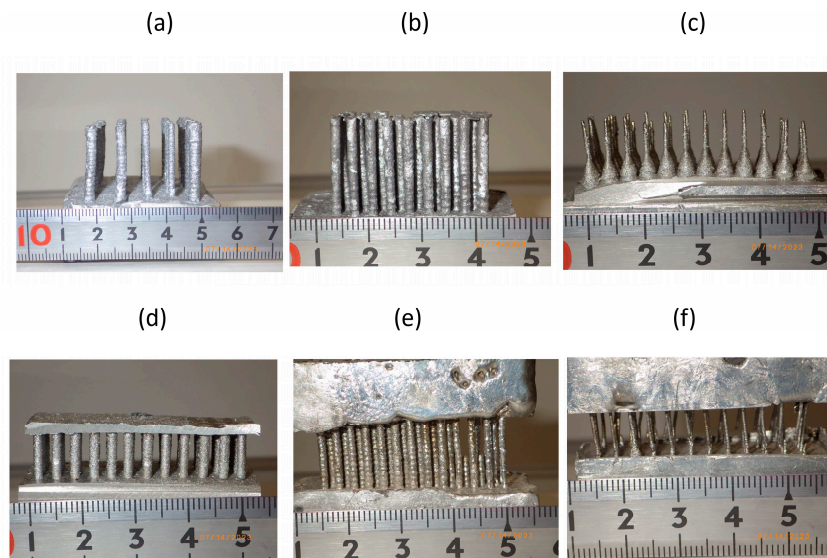


Figure 10. Various sizes of columnar-structured aluminum alloys. (a) Ten columns with a diameter of 2.0 mm, ten columns with a diameter of 3.0 mm, and five columns with a diameter of 3.6 mm. (b) Thirty-two columns with a diameter of 1.7 mm. (c) Forty-eight columns with a diameter of 0.6 mm. (d) Forty-eight columns with a diameter of 1.6 mm. (e) Sixty-three columns with a diameter of 1.5 mm. (f) Forty-eight columns with a diameter of 0.7 mm.

3.3. Removal of Ceramic Fiber

In the fabrication of the columnar-structured aluminum alloy, the cores play a major role as the matrix, while aluminum alloy plays a minor role. After casting, the majority of the cores is easily removed by immersing them in water. Figure 11a shows the ceramic fiber core absorbed water and was macerated to become sodden. After the core was removed, a columnar-structured aluminum alloy was fabricated, as shown in Figure 11b. The columns consisted of 10 columns with a diameter of 2.0 mm, 10 columns with a diameter of 3.0 mm, and 5 columns with a diameter of 3.6 mm. Since all columnar diameters were larger than 2.0 mm, the vacuum suction casting method was not adopted.

On the other hand, in the fabrication of the open-channel aluminum alloy, it is necessary to extract the reinforced materials, such as plates or wires, that were coated with the adhesive and the mixture of disassembled ceramic fiber and polyvinyl alcohol. The feasibility of extracting the templates is expressed in terms of the extraction force, which is equivalent to the tensile force in the stress–strain curve in the tensile test. This extraction force does not accompany plastic deformation, which is, in other words, the tensile force in the range of elastic deformation. Figure 12 shows an example of the tensile test to pull the reinforced wire of 0.97 mm in diameter and 75 mm in length from the aluminum alloy. These wires were coated with the mixture of disassembled fibers impregnated with polyvinyl alcohol. Figure 13 shows plots of the extraction force versus extraction length of the reinforced wire whose surface was coated with the adhesive and the mixture of ceramic fiber and polyvinyl alcohol. In the extraction process, the wire was pulled out by sliding along the hole without severe friction so that the extraction force almost kept constant. The extraction forces are very small, evaluated as 0 to 5 N. It is known that a wire with an extraction force of less than about 50N can be extracted manually. Thus, the reinforced wire

can be pulled out by hand. This is advantageous; the tensile machine is not necessary, and the procedure for the removal of the template materials becomes simple and time-saving with low cost performance.

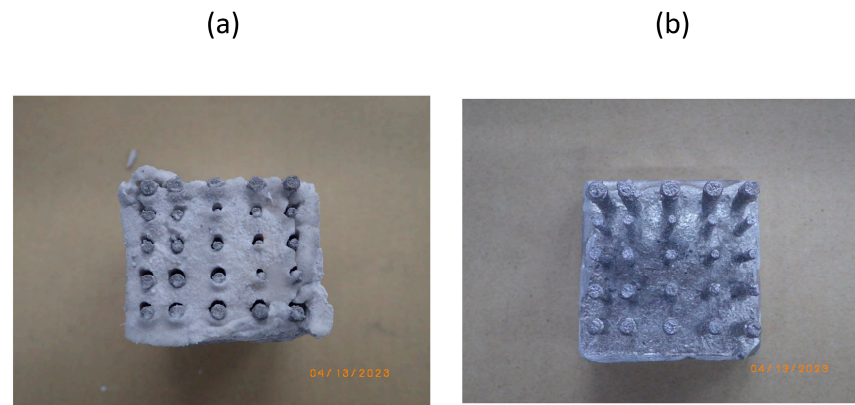


Figure 11. (a) Water-absorbed ceramic fiber core and (b) columnar-structured aluminum alloy fabricated by the ceramic fiber template method.



Figure 12. Extraction process of SUS wire coated with the mixture of disassembled fibers and polyvinyl alcohol. SUS wire: 0.97 mm in diameter and 75 mm in length.

3.4. Comparison of Fiber Template Method with Previous Investigations

As discussed in the Introduction, there are several manufacturing methods available. Steel or aluminum wires embedded in cold-pressed copper or titanium alloy powders can be removed by chemical or electrochemical dissolution. Steel wires embedded in solidified aluminum alloys can be removed by the extraction of the wires in semisolids or solids. One of the promising methods of the removal of templates is the extraction of wires at room temperature [30]. Therefore, it is worthwhile to compare the ceramic fiber method with a method of wire extraction at room temperature.

In the wire-extraction method, wires were coated with lubricant and embedded in a melt of metal. After solidification, the wires were extracted by tensile force; the wires were pulled out by a tensile machine. Since holes are formed by the removal of the wires, open-channel metals can be fabricated. Figure 14a shows the extraction force versus extraction length curve of a wire uncoated with lubricant. The SUS wires were alloyed with aluminum during melting so that the wires could not be extracted. The wire was fractured due to large tensile forces. The upper curve in Figure 14b shows the extraction force versus extraction length of a wire coated with boron nitride. The wire was extracted with a small extraction force, which suggests that boron nitride serves as a lubricant and a barrier of diffusion

between stainless steel and the aluminum alloy, and the alloying process is suppressed. This is why it is possible to extract the wires. Furthermore, the addition of MgH_2 to boron nitride decreases the extraction force, as depicted by the lower curve in Figure 14b. It was shown that the decrease in the extraction force is attributed to the formation of porous layers between the template's stainless steel wires and the aluminum alloy [31].

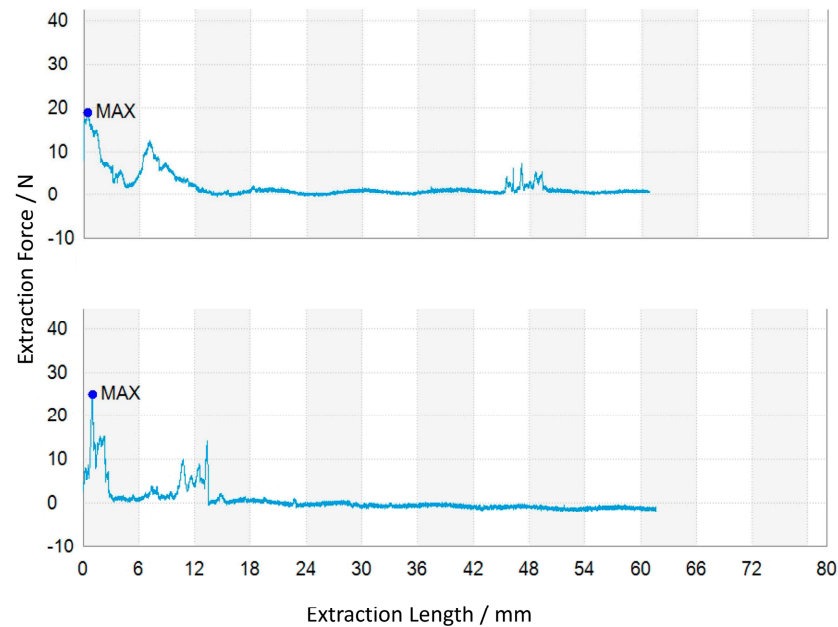


Figure 13. Extraction force–extraction length curves of SUS wires coated with the mixture of disassembled fibers and polyvinyl alcohol. SUS wire: 0.97 mm in diameter and 75 mm in length.

(a)

(b)

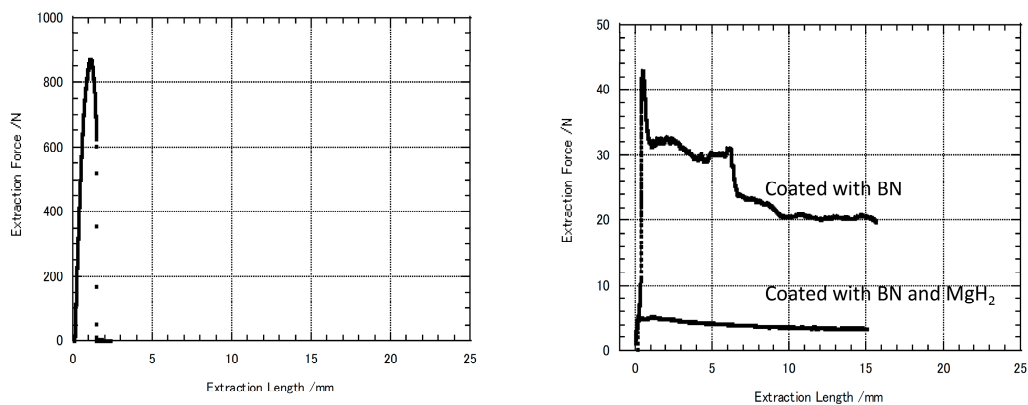


Figure 14. (a) Extraction force–extraction length curve of SUS wire of 1.0 mm embedded in aluminum, (b) extraction force–extraction length curve of SUS wire coated with BN, and extraction force–extraction length curve of SUS wire coated with a mixture of BN and MgH_2 [31].

Furthermore, Figure 15a,b shows the dependence of the extraction force of SUS template wires on the template length and the diameter, respectively. The SUS wires were coated with the mixture of BN and MgH_2 with a weight ratio of $W_{MgH_2}/W_{BN} = 1.5$. The extraction force of wires was decreased owing to the addition of MgH_2 . In the measurement of the result described in Figure 15a, the template diameter was kept constant at 1.0 mm, while in the measurement of Figure 15b, the template length was kept constant at 40 mm. The extraction force is directly proportional to the length of the wires, and the extraction

force increases linearly with an increase in the diameter of the wires. Taking these results into consideration, the increase in the contact area of the wires to the aluminum alloy increases the extraction force because of the increase in the friction force between them.

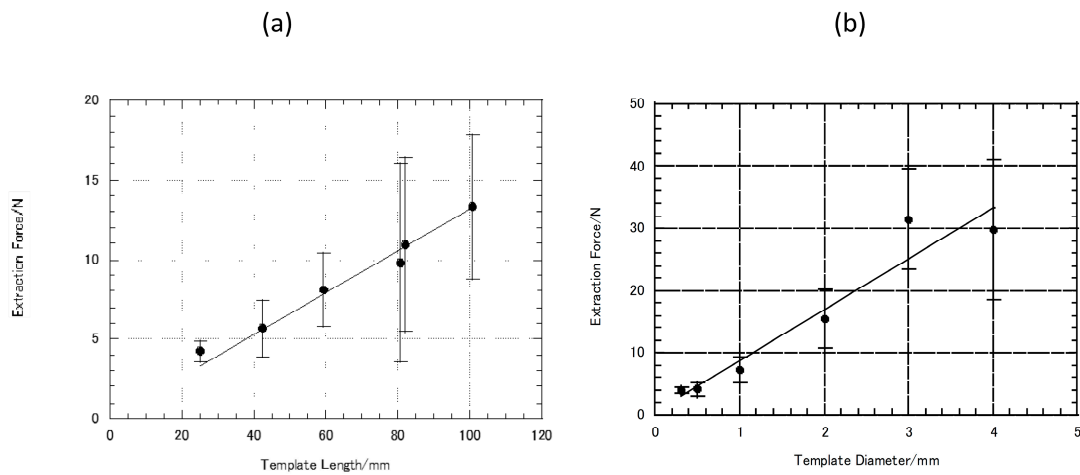


Figure 15. (a) Variation of extraction force with SUS wire length of open-channel aluminum fabricated by the wire-extraction method. (b) Variation of extraction force with SUS wire diameter of open-channel aluminum fabricated by the wire-extraction method [31].

On the other hand, in the ceramic fiber method, the mixture of ceramic fiber and polyvinyl alcohol is coated on the metallic plates or wires. The removal of the templates is carried out by dissolution of the mixture. Thus, the mechanism of the fiber template method is apparently different from that of the wire-extraction method. The former needs only water to dissolve the templates, while the latter needs mechanical strength.

Finally, we can estimate the magnitude of the extraction force F necessary to extract SUS wires by the wire-extraction method and the fiber template method on the basis of the data of Figure 15a,b. Let us take an open-channel heat sink as an example, which is illustrated in Figure 16a. The main body of the heat sink is an open-channel aluminum alloy, AC4CH, which was fabricated by the fiber template method. The thickness and length are 2.0 mm in diameter and 50.0 mm long, respectively, as shown in Figure 16b,c. A heat sink is a passive heat exchanger that transfers the heat generated by an electronic or a mechanical device to a fluid medium, often air or a liquid coolant, where it is dissipated away from the device, thereby allowing regulation of the device's temperature. Heat sinks are designed to maximize their surface area in contact with the cooling medium surrounding them [36,37].

If the open-channel aluminum alloy is fabricated by the wire-extraction method, the extraction force F can be predicted on the basis of the result in Figure 15a,b. We can see that F increases by 1.4 times from $L = 40$ mm to $L = 50$ mm, while F increases by 2.0 times from $d = 1.0$ mm to $d = 2.0$ mm. It is known that F is 43 N when an SUS wire of 40 mm in length and 1.0 mm in diameter is extracted. Thereby, the value of F of a SUS wire of 50 mm in length and 2.0 mm in diameter is evaluated to be $1.4 \times 2.0 \times 43$ N = 120.4 N. If 20 wires are extracted simultaneously, F amounts to $120.4 \times 20 = 2408$ N. On the other hand, when the open-channel aluminum alloy is fabricated by the fiber template method, F is as much as 3 N. If 20 wires are extracted simultaneously, F is estimated to be only 3 N \times $20 = 60$ N, which is 1/40 times smaller than that of the wire-extraction method. Remember that 60 N is the force by which the wires can be removed smoothly by hand. This is a significant contrast to the wire-extraction method. Thus, it is concluded that the fiber template method is the most superior production technique, with merits of low cost and time-saving performance.

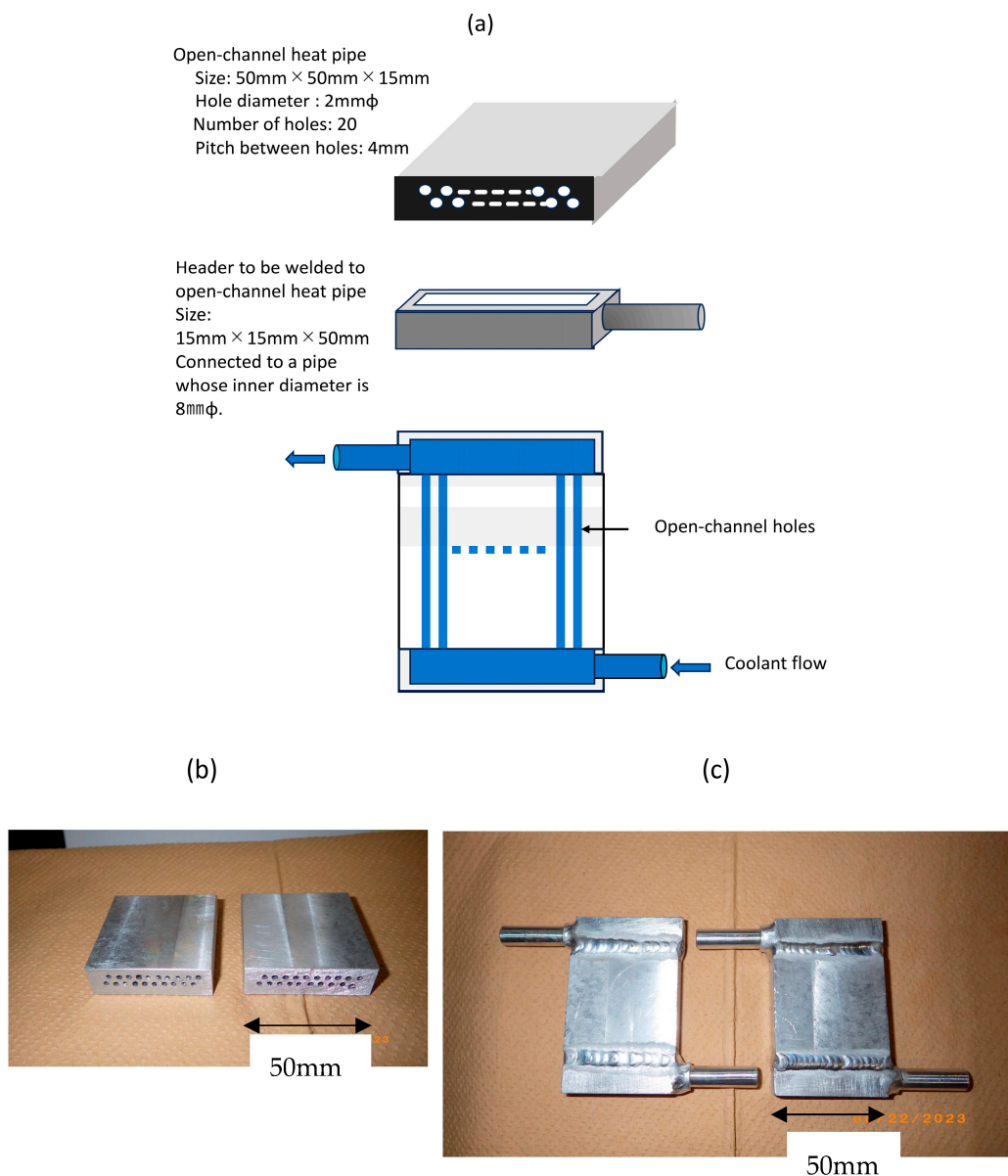


Figure 16. (a) Schematic drawing of open-channel heat sink and header, (b) open-channel aluminum alloy AC4CH for heat sinks, and (c) open-channel heat sinks welded with headers.

The difference in manufacturing techniques between the wire-extraction method and fiber template method is discussed and tabulated in Table 2. The most remarkable difference between the wire-extraction method and fiber template method is in the removal of the templates. The latter exhibits superior cost performance and a more time-saving procedure. A difference between the use case of the reinforced metals and the use case of drilled holes is also noticed. The former needs metallic wires or plates to reinforce the templates, while the latter does not.

Table 2. Comparison of manufacturing techniques.

Process	Wire-Extraction Method	Fiber Template Method	
Fabricated structure	Open-channel	Open-channel	Columns
Template	Wires coated with lubricant	Reinforced plate or wire coated with fiber + PVA	Drilled hole perforated in fiber + PVA
Casting process	Embedded in aluminum alloy melt		
Removal of templates	Extraction by tensile machine	Impregnated by water	
Roughness of inner wall	Not controllable	Controllable	
Cost performance	Not good	Good	

PVA: polyvinyl alcohol.

Furthermore, in the wire-extraction method, the significant roughness of the coated wires makes the smooth extraction of the wires difficult because of the increase in the friction between the wires and aluminum alloy. The roughness cannot be controlled. On the other hand, in the fiber template method, holes with various height of roughness can be fabricated because the templates can be removed by maceration due to water. In some cases, a rough inner wall inside the holes is favorable. For example, if the surface of heat sinks in contact with hot or cold fluid is rough, the heat transfer increases, since the surface area increases. As a result, the roughness can be adjusted in order to obtain better performance, such as improved thermal properties, in the fiber template method.

As mentioned above, the fiber template method differs from the wire-extraction method in the mechanism each uses. In order to clarify the difference of both methods, the volume change of the cores before and after casting was evaluated. For example, in the fiber template method, fibers with a thickness of 0.27 mm were coated on an SUS wire with a diameter of 1.96 mm. After casting, the fiber layer shrunk to a diameter of 2.13 mm, and the core volume decreased by 0.7, as shown in Figure 8.

On the other hand, in the wire-extraction method, two methods are shown here. Schematic drawings of the cross-sections of the cores are illustrated in Figure 17. First, boron nitride with a thickness of 0.05 mm was coated on the SUS wires with a diameter of 1.08 mm. After casting, the boron nitride layer did not change. Secondly, a mixture of boron nitride and magnesium hydride with a thickness of 0.05 mm was coated on SUS wire with a diameter of 1.08 mm. After casting, the layer swelled to a diameter of 1.45 mm, and the core volume increased by 1.5. Thus, the change in the core volume in both methods is clearly different before and after casting; the coated layers decrease in volume in the fiber template method, while they increase in volume in the wire-extraction method.

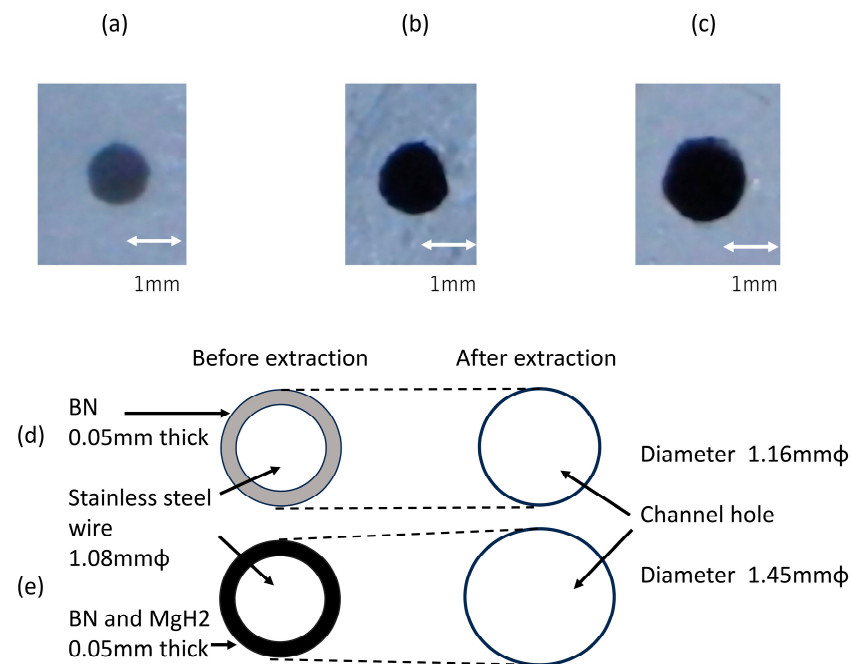


Figure 17. (a) Cross-sectional view of SUS wire embedded in aluminum. (b) Cross-sectional view of a channel hole perforated by the extraction of SUS wire coated with BN. (c) Cross-sectional view of a channel hole perforated by the extraction of SUS wire coated with BN and MgH₂. (d) Schematic drawing of a section of a channel hole extracted by SUS wire coated with BN, and (e) schematic drawing of a section of a channel hole extracted by SUS wire coated with BN and MgH₂ [31].

4. Conclusions

Aluminum alloys with open-channel and columnar structures are fabricated by casting a melt of aluminum alloys using a ceramic fiber template method in the present research. It is known in the wire-extraction method that open-channel aluminum alloys can be fabricated by the removal of template wires that were embedded in the aluminum alloy. A large extraction force is indispensable to extract many wires simultaneously to produce open-channel aluminum alloys with many directional holes. The process is laborious and time-consuming and is therefore not suitable for mass production. A simple manufacturing technique is desirable.

The present research proposes a novel “ceramic fiber template method” to fabricate open-channel aluminum alloys. Instead of metallic wires, fibers solidified with polyvinyl alcohol are used as the templates. It is found that the fibers embedded in cast aluminum alloys are easily removed by water, so the use of an extraction force is not necessary, which give benefits in terms of the time-saving and low-cost mass production of open-channel aluminum alloys. Furthermore, columnar-structured aluminum alloys are also fabricated using the fiber template method. Open-channel aluminum alloys fabricated by this method are expected to be used for high-performance heat sinks, heat exchangers, etc.

Funding: This research received no external funding.

Data Availability Statement: Data is contained within the article.

Conflicts of Interest: The author declares that there is no known competing financial interest or personal relationships that could have appeared to influence the work reported in this paper. Hideo Nakajima was employed by the company Institute for Lotus Materials Research Co., Ltd. and Sumitomo Precision Products Co., Ltd.

References

1. Gibson, L.J.; Ashby, M.F. *Cellular Solids*; Cambridge University Press: Cambridge, UK, 1997.
2. Nakajima, H. Fabrication, properties and application of porous metals with directional pores. *Prog. Mater. Sci.* **2007**, *52*, 1091–1173. [[CrossRef](#)]
3. Drenchev, L.; Sobczak, J.J. *GASARS—A Special Class of Porous Materials*; Motor Transport Institute, Warsaw and Foundry Research Institute: Cracow, Poland, 2008.
4. Gibson, L.J.; Ashby, M.F.; Harley, B.A. *Cellular Materials in Nature and Medicine*; Cambridge University Press: Cambridge, UK, 2010.
5. Chiba, H.; Ogushi, T.; Nakajima, H. Heat transfer capacity of lotus-type porous copper heat sink for air cooling. *J. Thermal Sci. Technol.* **2010**, *5*, 222–237. [[CrossRef](#)]
6. Ikeda, T.; Aoki, T.; Nakajima, H. Fabrication of lotus-type porous stainless steel by continuous zone melting technique and mechanical property. *Metall. Mater. Trans.* **2005**, *36A*, 77–86. [[CrossRef](#)]
7. Zhou, C.; Liu, Y.; Zhang, H.; Chen, K.; Li, Y. Compressive and corrosion properties of lotus-type porous Mg-Mn alloys fabricated by unidirectional solidification. *Metall. Mater. Trans.* **2020**, *51A*, 3238–3247. [[CrossRef](#)]
8. Liu, X.; Li, Y.; Zhang, H.; Liu, Y.; Chen, X. Pore structure analysis of directionally solidified porous copper. *China Foundry* **2020**, *17*, 325–331. [[CrossRef](#)]
9. Liu, E.; He, P.; Li, Z.; Wu, C.; Liu, M. Fabrication of gasar porous Mg-Ag alloys by metal-gas eutectic directional solidification method. *Cryst. Growth Des.* **2023**, *23*, 8303–8310. [[CrossRef](#)]
10. Sadeghi, Z.; Mansoorianfar, M.; Panjepour, M.; Meratian, M. Lotus-type porous magnesium production via in situ pyrolysis of viscose rayon fiber in a melting process. *J. Mater. Sci.* **2023**, *58*, 9297–9307. [[CrossRef](#)]
11. Utsunomiya, H.; Koh, H.; Miyamoto, J.; Sakai, T. High-strength porous copper by cold-extrusion. *Adv. Eng. Mater.* **2008**, *10*, 826–829. [[CrossRef](#)]
12. Vesenjajak, M.; Nakashima, Y.; Hokamoto, K.; Ren, Z.; Marumo, Y. Development of unidirectional cellular structure with multiple pipe layers and characterisation of its mechanical properties. *Materials* **2020**, *13*, 3880. [[CrossRef](#)]
13. Nishi, M.; Tanaka, S.; Vesenjajak, M.; Ren, Z.; Hokamoto, K. Experimental and computational analysis of the uni-directional porous (UniPore) copper mechanical response at high-velocity impact. *Inter. J. Impact Eng.* **2020**, *136*, 103409. [[CrossRef](#)]
14. Ide, T.; Iio, Y.; Nakajima, H. Fabrication of porous aluminum with directional pores through continuous casting technique. *Metall. Mater. Trans.* **2012**, *43A*, 5140–5152. [[CrossRef](#)]
15. Takahashi, K.; Sasajima, Y.; Ikeda, T. Pore formation and shape control simulation of lotus aluminum by the phase-field method. *ACS Omega* **2022**, *7*, 14985–14993. [[CrossRef](#)] [[PubMed](#)]
16. Goto, Y. Available online: <http://www.osaka-jp.net/osk22-2.htm> (accessed on 12 October 2023).
17. Gillen, D.; Moore, D. Available online: <http://www.blueacretchnology.com> (accessed on 12 October 2023).
18. Gregory, O.; Griffith, A.J.; Stroud, D. Drilling Turbine Blades. U.S. Patent 5,222,617, 29 June 1993.
19. Hakamada, M.; Asao, Y.; Kuromura, T.; Chen, Y.; Kusuda, H.; Mabuchi, M. Processing of three-dimensional metallic microchannel by spacer method. *Mater. Lett.* **2008**, *62*, 1118–1121. [[CrossRef](#)]
20. Kwok, P.J.; Oppenheimer, S.M.; Dunand, D.C. Porous titanium by electro-chemical dissolution of steel space-holders. *Adv. Eng. Mater.* **2008**, *10*, 820–825. [[CrossRef](#)]
21. Jorgensen, D.J.; Dunand, D.C. Structure and mechanical properties of Ti-6Al-4V with a replicated network of elongated pores. *Acta Mater.* **2011**, *59*, 640–650. [[CrossRef](#)]
22. Neurohr, A.J.; Dunand, D.C. Shape-memory NiTi with two-dimensional networks of micro-channels. *Acta Biomater.* **2011**, *7*, 1862–1872. [[CrossRef](#)]
23. Haga, T.; Toyoda, K.; Fuse, H. Effect of casting conditions on fabrication of lotus type holes in ingot cast by core-bar pulling method. *Key Eng. Mater.* **2017**, *748*, 187–191. [[CrossRef](#)]
24. Haga, T.; Fuse, H. Fabrication of lotus type through-holes using the semisolid condition. *Adv. Mater. Process. Tech.* **2018**, *4*, 16–23. [[CrossRef](#)]
25. Haga, T.; Fuse, H. Fabrication of lotus type porous ingots using the core-bar pulling method. *Solid State Phenom.* **2019**, *285*, 259–263. [[CrossRef](#)]
26. Muto, D.; Yoshida, T.; Tamai, T.; Sawada, M.; Suzuki, S. Fabrication porous metals with unidirectionally aligned pores by rod-dipping process. *Mater. Trans.* **2019**, *60*, 544–553. [[CrossRef](#)]
27. Sawada, M.; Ichikawa, D.; Borovinsek, M.; Vesenjajak, M.; Suzuki, S. Characterization of the compressive stress drop in the plateau region in porous metals with unidirectional pores. *Mater. Trans.* **2020**, *61*, 1782–1789. [[CrossRef](#)]
28. Ichikawa, D.; Sawada, M.; Suzuki, S. The compression angle dependence of the strength of porous metals with regularly aligned directional pores. *Mater. Trans.* **2023**, *64*, 2471–2480. [[CrossRef](#)]
29. Kaneko, A.; Takeuchi, G.; Abe, Y.; Suzuki, Y. Condensation behavior in a microchannel heat exchanger. *J. Thermal Sci. Tech.* **2009**, *4*, 469–482. [[CrossRef](#)]
30. Nakajima, H. Through Hole Aluminum Fabricated by the Extraction of Lubricated Metallic Wires. *Metall. Mater. Trans.* **2019**, *50A*, 5707–5712. [[CrossRef](#)]
31. Nakajima, H. Fabrication of open-channel aluminum by template-extraction technique. *Mater. Trans.* **2023**, *64*, 2643–2647. [[CrossRef](#)]

32. Triyono, T.; Muhayat, N.; Supriyanto, A.; Lutiyaatmi, L. Effect of degassing treatment on the interfacial reaction of molten aluminum and solid steel. *Arch. Foundry Eng.* **2017**, *17*, 227–239. [[CrossRef](#)]
33. Lazaro-Nebreda, J.; Patel, J.B.; Lordan, E.; Zhang, Y.; Karakulak, E.; Al-Helal, K.; Scamans, G.M.; Fan, Z. Degassing of aluminum alloy melts by high shear melt conditioning technology: An overview. *Metals* **2022**, *12*, 1772. [[CrossRef](#)]
34. Hayashi, Y. Suction die casting process. *J. Jpn. Foundrymen's Soc.* **1994**, *66*, 955–960. (In Japanese)
35. Szklarz, Z.; Krawiec, H.; Rogal, L. The effect of vacuum suction casting on the microstructure and corrosion behavior of aluminium alloy 2017. *Mater. Sci. Eng. B* **2019**, *240*, 23–32. [[CrossRef](#)]
36. Kadam, S.T.; Kumar, R. Twenty first century cooling solution: Microchannel heat sinks. *Int. J. Therm. Sci.* **2014**, *85*, 73–92. [[CrossRef](#)]
37. Zhou, J.; Cao, X.; Zhang, N.; Yuan, Y.; Zhao, X.; Hardy, D. Micro-channel heat sink: A review. *J. Therm. Sci.* **2020**, *29*, 1431–1462. [[CrossRef](#)]

Disclaimer/Publisher's Note: The statements, opinions and data contained in all publications are solely those of the individual author(s) and contributor(s) and not of MDPI and/or the editor(s). MDPI and/or the editor(s) disclaim responsibility for any injury to people or property resulting from any ideas, methods, instructions or products referred to in the content.